Faculty Publications

7-1-2014

Gelatinous Zooplankton Biomass In the Global Oceans: Geographic Variation and Environmental Drivers

Cathy H. Lucas
University of Southampton, cathy.lucas@noc.soton.ac.uk

Daniel O.B. Jones
University of Southampton

Catherine J. Hollyhead
University of Southampton

Robert H. Condon
University of North Carolina Wilmington, rcondon@disl.org

Carlos M. Duarte
CSIC-UIB - Instituto Mediterraneo de Estudios Avanzados (IMEDEA), carlos.duarte@uwa.edu.au

See next page for additional authors

Follow this and additional works at: https://aquila.usm.edu/fac_pubs

Part of the Ecology and Evolutionary Biology Commons

Recommended Citation

Authors

Cathy H. Lucas, Daniel O.B. Jones, Catherine J. Hollyhead, Robert H. Condon, Carlos M. Duarte, William M. Graham, Kelly L. Robinson, Kylie A. Pitt, Mark Schildhauer, and Jim Regetz

1 Gelatinous zooplankton biomass in the global ocean: geographic variation

2 and environmental drivers

3

4

5 Cathy H. Lucas[1,#], Daniel O. B. Jones[1], Catherine J. Hollyhead[1,2], Robert H.

6 Condon[3], Carlos M. Duarte[4,5,6], William M. Graham[7], Kelly L. Robinson[7], Kylie

7 A. Pitt[8], Mark Schildhauer[9], Jim Regetz[9]

8

9

10 [1] National Oceanography Centre, University of Southampton Waterfront Campus, European

11 Way, Southampton, SO14 3ZH, UK

12 cathy.lucas@noc.soton.ac.uk

13 dj1@noc.ac.uk

14

15 [2]Civil, Maritime and Environmental Engineering and Science Unit, University of

16 Southampton, Highfield, Southampton SO17 1BJ, UK.

17 cjh1g08@soton.ac.uk

18

19 [3]University of North Carolina Wilmington, Department of Biology and Marine Biology, 601

20 S. College Road, Wilmington NC, 28403, USA.

21 condonr@uncw.edu

22

23 [4]Department of Global Change Research, Instituto Mediterráneo de Estudios Avanzados

24 IMEDEA (UIB-CSIC), Esporles, Spain.

25

26 [5]The UWA Oceans Institute, The University of Western Australia, M470, 35 Stirling

27 Highway, Crawley WA 6009 Australia.

28 carlos.duarte@uwa.edu.au

29

30 [6]Faculty of Marine Sciences, King Abdulaziz University, P. O. Box 80207, Jeddah 21589

31 Saudi Arabia

32

33 [7]Department of Marine Science, The University of Southern Mississippi, 1020 Balch Blvd.,

34 Stennis Space Center, MS 39529, USA.

35 Monty.Graham@usm.edu

36 Kelly.L.Robinson@usm.edu

37

38 [8]Australian Rivers Institute and Griffith School of Environment, Griffith University,

39 Gold Coast Campus, QLD 4111, Australia.

40 k.pitt@griffith.edu.au

41

42 [9]National Center for Ecological Analysis and Synthesis (NCEAS), 735 State Street, Santa

43 Barbara, CA 93101, USA.

44 schild@nceas.ucsb.edu

45 regetz@nceas.ucsb.edu

46

47

48

49 #Correspondence: Cathy Lucas: National Oceanography Centre, University of Southampton

50 Waterfront Campus, European Way, Southampton, SO14 3ZH, UK.

51 cathy.lucas@noc.soton.ac.uk

52

53

54 **Article type:** Research paper

55

56 **Keywords:** Cnidaria, Ctenophora, Thaliacea, jellyfish blooms, JEDI, global ocean,

57 geographic trends, environmental drivers, macroecology.

58

59 **Running title:** Global gelatinous biomass

60

61 **Abstract word count:** 299; **Text word count:** 5030

62   **ABSTRACT**

63   **Aim:** Scientific debate regarding future trends, and subsequent ecological, biogeochemical

64   and societal impacts, of gelatinous zooplankton (GZ) in a changing ocean is hampered by

65   lack of a global baseline and understanding of the causes of biogeographic patterns. We

66   address this using a new global database of GZ records to test hypotheses relating to

67   environmental drivers of biogeographic variation in the multi-decadal baseline of epipelagic

68   GZ biomass in the world's oceans.

69   **Location:** Global ocean.

70   **Methods:** Over 476,000 global GZ data and metadata were assembled from a variety of

71   published and unpublished sources. From this, a total of 91,765 quantitative abundance data

72   from 1934 to 2011 were converted to carbon biomass using published biometric equations

73   and species-specific average sizes. Total GZ, Cnidaria, Ctenophora and Chordata (Thaliacea)

74   biomass was mapped into 5° grid cells and environmental drivers of geographic variation

75   tested using spatial linear models.

76   **Results:** We present JeDI (Jellyfish Database Initiative), a publically accessible database

77   available at http://jedi.nceas.ucsb.edu. We show that: (1) GZ are present throughout the

78   world's oceans; (2) global geometric mean and standard deviation of total gelatinous biomass

79   is 0.53 ± 16.16 mg C m^{-3}, corresponding to a global biomass of 38.3 Tg C in the mixed layer

80   of the ocean; (3) biomass of all gelatinous phyla is greatest in the subtropical and boreal

81   Northern Hemisphere; and (4) within the North Atlantic, dissolved oxygen, apparent oxygen

82   utilisation and sea surface temperature are the principal drivers of biomass distribution.

83   **Main conclusions:** JeDI is a unique global dataset of GZ taxa, which will provide a

84   benchmark against which future observations can be compared and shifting baselines

85   assessed. The presence of GZ throughout the world's oceans and across the complete global

86   spectra of environmental variables indicates that evolution has delivered a range of species

87   able to adapt to all available ecological niches.

88

89   **INTRODUCTION**

90   Global climate change and anthropogenic activities are changing the ecology and

91   biogeography of populations inhabiting the world's oceans, with effects likely to be greatest

92   in the high latitudes of the Northern Hemisphere (IPCC, 2007; Jones *et al.*, in press).

93   Empirical evidence indicates that such changes will significantly impact marine ecosystems

94   and associated ecosystem services including fisheries (Cheung *et al.*, 2010). By

95   understanding the relationships between biodiversity and biomass, and their biotic and abiotic

96   drivers, we can begin to predict ecosystem response to future scenarios of climate change,

97   human impact and habitat loss (Cheung *et al.*, 2008; Beaugrand *et al.*, 2010). These

98   relationships are well-established for terrestrial ecosystems (Hendriks *et al.*, 2006; Robinson

99   *et al.*, 2011), but there are far fewer such studies in marine ecosystems owing to the extensive

100 spatiotemporal variability of the oceans and limited availability of robust data for many

101 marine taxa, particularly for the open ocean, deep sea, and the Southern Hemisphere (but see

102 Beaugrand *et al.*, 2010; Tittensor *et al.*, 2010). Additionally, spatial patterns and drivers of

103 biomass are particularly understudied, with fewer established patterns compared with those

104 for biodiversity. Whereas plant biomass (Hese *et al.*, 2005) and production (Field *et al.*,

105 1998) can be resolved from remotely-sensed products, allowing for global patterns to be

106 examined (Huston & Wolverton, 2009), animal biomass is more elusive. On land, global

107 patterns of animal abundance have been derived to test hypotheses on the allometric scaling

108 of population energy use (Currie & Fritz, 1993), and the drivers of global biomass patterns

109 have also been evaluated for microbial and faunal belowground communities (Fierer *et al.*,

110 2009). Macroecology, life-history theory and food-web ecology were used to predict global

111   production and biomass of marine animals (Jennings *et al.*, 2008) with highest teleost fish

112   biomass reported for productive, cooler upwellings and mid-latitude shelf seas. Food

113   availability influences spatial patterns of global zooplankton biomass (Hernández-León &

114   Ikeda, 2005) and deep-sea benthic biomass (Wei *et al.*, 2010), and bathymetric changes in the

115   biomass of deep-sea benthos have also been characterized at the global scale (Rex *et al.*,

116   2006). In the more physically-complex and variable sedimentary and rocky intertidal habitats,

117   grain size and wave exposure, respectively are the best predictors of macroinvertebrate

118   biomass (Ricciardi & Bourget, 1999).

119

120   Marine zooplankton are crucial for ecosystem function and biogeochemical cycling, linking

121   primary production to higher trophic levels and deep sea communities, and acting as

122   hydroclimatic indicators (Richardson, 2008). Gelatinous taxa within the Cnidaria,

123   Ctenophora, and Chordata (Thaliacea), herein referred collectively as gelatinous zooplankton

124   (GZ), are ubiquitous members of zooplankton communities and important consumers on

125   basal production, both as grazers of phytoplankton (thaliaceans) and predators of

126   zooplankton, fish larvae and other GZ (medusae and ctenophores). They can rapidly

127   reproduce and form blooms under suitable environmental conditions, and have been widely

128   reported to have negative ecological and socio-economic impacts: reducing commercially-

129   harvested fish stocks (Pauly *et al.*, 2009), limiting bioavailable carbon to higher trophic levels

130   and promoting microbially-mediated food webs (Condon *et al.*, 2011), and causing

131   detrimental economic impacts on aquaculture, tourism and coastal infrastructure (Purcell *et*

132   *al.*, 2007). Nonetheless, GZ provide a vital food source for critically-endangered charismatic

133   species such as the Leatherback turtle *Dermochelys coriacea*, and may even influence their

134   distribution (Houghton *et al.*, 2006). Additionally, post-bloom jelly-falls may accelerate the

135   biological pump and increase carbon sequestration from the upper ocean to the deep sea-floor

136   (Lebrato *et al.*, 2012).

137

138   Fossil evidence and evolutionary supposition indicate cnidarians and ctenophores have

139   existed for over 500 million years during which they have independently adapted to the major

140   global climate cycles of warming and cooling and changes in oceanic and atmospheric

141   conditions; in line with paleoecological insights of long-term resilience for terrestrial species

142   (Moritz & Agudo, 2013). A recent study has reported increases in regional and global

143   populations of GZ over decadal timescales (Brotz *et al.*, 2012), although Condon *et al*. (2013)

144   suggest that GZ blooms display predictable periodic or decadal fluctuations rather than a

145   sustained monotonic increase. Insufficient long-term quantitative datasets and the lack of a

146   defined global baseline of gelatinous biomass has been a major limitation to substantiate this

147   concept. Historically, complete estimation of gelatinous biomass has been hindered by

148   sampling difficulties associated with their extreme fragility, seasonal periodicity, physical

149   aggregation and blooming tendencies, paucity of samples from the much of the open ocean

150   and sampling approaches biased toward non-gelatinous taxa. Recent advances have alleviated

151   some of these problems; hence, a composite of data sources on GZ abundance have become

152   available from across the ocean, offering an opportunity to examine the global distribution of

153   biomass for future reference.

154

155   The aims of this paper are to (1) define global baselines of carbon biomass for the Cnidaria,

156   Ctenophora, Chordata (Thaliacea) and total GZ (all 3 phyla combined) within the epipelagic

157   ocean; (2) identify geographic trends in global GZ biomass by latitude and Longhurst

158   biogeochemical province; and (3) explore the principal underlying oceanic and environmental

159   drivers of spatial variation in Cnidaria, Ctenophora and Thaliacea mean biomass, with

160   predictor variables chosen on the basis of published studies. As temperature and food

161   availability are considered to be the most important variables structuring marine ecosystems

162   (Jennings *et al.*, 2008; Richardson, 2008) we specifically test *a priori* the following

163   hypotheses relating to biogeographic distribution of gelatinous biomass: 1) GZ biomass is

164   positively correlated with sea surface temperature, and 2) GZ biomass is greater in regions

165   characterised by high primary production. Through these efforts we attempt to take a step

166   towards bridging the current gap between the development of global ecology and

167   biogeography on land and that at sea; a gap that reflects the much lower research effort, about

168   10%, in the later domain despite the oceans covering 71% of our planet (Hendriks *et al.*,

169   2006).

170

171   **METHODS**

172   **The <u>J</u>ellyfish <u>D</u>atabase <u>I</u>nitiative (JeDI)**

173   JeDI is a scientifically-coordinated global jellyfish database housed at the National Center for

174   Ecological Analysis and Synthesis (Santa Barbara, CA), currently holding over 476,000

175   quantitative, categorical, presence-absence and presence only data on GZ spanning the past

176   four centuries (Appendix S1) (see Condon *et al.*, 2012). GZ data are reported to species level,

177   where identified, but phylum, family and order taxonomic information are reported for all

178   records. Other auxiliary metadata, such as physical, environmental and biometric information

179   relating to the GZ metadata, are included with each respective JeDI entry (Appendix S2).

180   JeDI has also been constructed as a future repository of datasets, and metadata and raw data

181   can be accessed and searched at http://jedi.nceas.ucsb.edu.

182

183   **Treatment of JeDI and environmental data**

184   Quantitative numerical abundance data (no. m^{-3}) of all GZ taxa in the upper 200 m, collected

185   using a number of sampling gears (Appendix S3), were extracted from JeDI between the

186   years 1934 and 2011. Abundance was converted into biomass (mg C m^{-3}) using species,

187   family or group-specific length-mass or mass-mass linear and logistic regression equations

188   (Lucas *et al.*, 2011). Average length measurements for each taxon were taken from the

189   SeaLifeBase database (www.sealifebase.org), with taxonomic verification provided by the

190   Catalogue of Life (www.catalogueoflife.org). As biometric equations are not available for all

191   identified gelatinous taxa, conversions were based on family or class-level comparable

192   lengths, and where the species epithet was not provided, conversions were computed

193   assuming the organism belonged to the same genus as previously identified in the same

194   region. Thirty-three regression equations, representing 18 species of Thaliacea, two

195   Hydrozoa, seven Scyphozoa, one Nuda and five Tentaculata, were used for abundance to

196   biomass conversion of 122 species of GZ recorded in JeDI (Appendix S4).

197

198   Maps illustrating the spatial distribution of Cnidaria, Ctenophora, Chordata and total GZ

199   biomass in 5° x 5° grid cells were produced using ArcGIS v10 ESRI. The minimum number

200   of samples yielding statistically-robust results of the abundance of Cnidaria, Ctenophora,

201   Thaliacea and total GZ biomass in 5° grid cells was determined by a bootstrapping exercise

202   whereby ten 5° grid cells were chosen randomly from the 20% of regions with the highest

203   number of observations. One hundred replicate bootstrapping simulations were run per cell

204   and the number of observations sampled ranged from 1 - 70 at increasing increments of one

205   without data replacement. Owing to lack of data for the Ctenophora 1 - 20 observations were

206   evaluated. To determine the minimum sample size required to adequately characterize the

207   mean biomass for each cell, relative standard errors (RSE) were compared to the

208   bootstrapping sample size for each bootstrap run (Appendix S5). These comparisons showed

209   that the RSE decreased rapidly to below 50% after which it stabilised. Using an RSE <50%

210   as the criteria for adequacy and for consistency across all three taxa, the minimum number of

211   observations per grid cell that yielded robust results, while retaining sufficient data for

212   statistical analysis, was 20 data points per grid cell. Consequently, in the North Atlantic

213   (which contains 219 x 5° cells) 47 cells with <20 observations were removed from analysis,

214   leaving a total of 109 out of 156 x 5° cells with any data. Subsequent analysis used $\log_{10}$

215   transformed data and geometric means, to avoid the effect of extreme observations on the

216   error and further stabilise the variance of data within a cell.

217

218   For each grid cell, calculations of the arithmetic mean, standard deviation, geometric mean,

219   geometric standard deviation and coefficient of variation (CV) were computed following the

220   removal of grid cells containing '0' values. CV highlights areas of the global ocean where the

221   extent of variability with respect to the mean is greatest and may be used as an indicator of

222   bloom tendencies defined according to Condon *et al.* (2013). The geometric means were

223   assigned to their appropriate Longhurst province and ocean basin, using the equator as a

224   north-south divide. As data were highly skewed (Table 1), the arithmetic mean was deemed

225   to be an unreliable indication of central tendency and all further synthesis was performed on

226   the geometric mean.

227

228   Potential drivers of biomass patterns were chosen based on established hypotheses relating to

229   temperature (sea surface temperature, SST), productivity (primary production, PP;

230   chlorophyll *a*, euphotic depth, apparent oxygen utilisation, AOU), oxygen stress (dissolved

231   oxygen, DO), depth and proximity of coastline (bathymetric depth, distance from coast) that

232   are known to affect biodiversity and biomass in the marine environment (Tittensor *et al.*,

233   2010) including GZ. Salinity was not considered as many GZ species (particularly

10

234   cnidarians), are euryhaline (see Lucas & Dawson, 2014). Furthermore, productivity can be

235   used as an indirect indicator for nutrient availability, as jellyfish generally obtain inorganic

236   nutrients through trophic transfer rather than direct assimilation. This approach encompasses

237   hypotheses about eutrophication causing jellyfish blooms because jellyfish respond to

238   productivity caused by eutrophication rather than the nutrients per se. Environmental

239   parameters were obtained from web-based resources as follows: depth from the National

240   Geophysical Data Centre (NGDC)

241   (http://www.ngdc.noaa.gov/mgg/global/relief/ETOPO2/ETOPO2v2-2006/ETOPO2v2g/),

242   surface chlorophyll *a* and SST from the Aqua MODIS satellite

243   (http://oceancolor.gsfc.nasa.gov/), DO and AOU, as netCDF files, from NODC's World

244   Ocean Atlas 2009, then averaged for the upper 200m of the water column

245   (http://www.nodc.noaa.gov/OC5/WOA09/netcdf_data.html). Euphotic depth data were from

246   NASA GIOVANNI Ocean Color Radiometry - Water Quality Portal

247   (http://gdata1.sci.gsfc.nasa.gov/daac-bin/G3/gui.cgi?instance_id=WaterQuality). Primary

248   production data were annually-integrated PP, averaged for the years 2003-2011, calculated

249   with the VGPM algorithm (Behrenfeld & Falkowski, 1997) from MODIS data. Distance from

250   the coast was calculated from a vector coastline file (http://www.gadm.org/) using the

251   Euclidean Distance tool (spatial analyst extension) in ArcGIS v10. A full summary of GZ

252   biomass, relative contribution of Cnidaria, Ctenophora and Thaliacea to total GZ by

253   abundance and biomass, and average values of environmental parameters for each Longhurst

254   province is given in Appendix S6.

255

256   **Statistical analyses and modelling of data**

257   When modelling the relationship between environmental predictors and response variables,

258   spatial autocorrelation violates the assumptions of traditional statistical approaches (Tittensor

259   *et al.*, 2010). Spatial autocorrelation extends to the scale of ocean basins. For the Cnidaria,

260   semivariance increased linearly with distance, at least to a distance (lag) exceeding 5500 km,

261   suggesting spatial correlation existed at all scales investigated. For the Thaliacea and

262   Ctenophora a clear sill was reached, where semivariance stopped increasing, and model fits

263   suggested that this occurred at distances of 6670 and 3970 km respectively. This spatial

264   autocorrelation results in deflated estimates of variance and corresponding impacts on

265   inference, among other issues. As a result, variables were modelled and inference conducted

266   using both generalized-linear models (GLM) and multivariate spatial linear models (SLM).

267   Models were developed separately for three taxa (Cnidaria, Ctenophora and Thaliacea),

268   recognising the differing trophic levels and life history characteristics of the groups.

269   Following preliminary data exploration, a $\log_{10}$ transformation of the response variables was

270   selected to homogenise variances and normalise data. GLMs resulted in model residuals that

271   were spatially non-independent for all taxa in global analyses, and therefore SLM were used

272   for final inference.

273

274   Spatial analysis was performed using an error-spatial autoregressive (SAR) model (Dormann

275   *et al.*, 2007), which uses maximum-likelihood spatial autoregression. Neighbourhood

276   thresholds between 500 and 10,000 km were tested at 100 km intervals and the optimal

277   neighbourhood size for each taxon was selected by minimising the Akaike information

278   criterion (AIC) for the spatial null model (the model only retaining a spatial autocorrelation

279   term). Backward stepwise elimination of insignificant parameters was then used to determine

280   the minimum adequate model. The importance of individual predictors was assessed through

281   t-tests (GLM) and z-tests (SLM). Models were tested further by separately including

282   quadratic terms and interactions between terms; these did not significantly decrease the

283   deviance of the models compared with the simple models so were not explored further.

284   Statistical analysis was carried out using the R programming environment and spatial model

285   analyses were carried out using R package "spdep" (Bivand *et al.*, 2008). Owing to sparse

286   data in some areas of the world, the analysis was carried out for the North Atlantic only, an

287   area north of a line between Natal, Brazil, and Bolama, Guinea-Bissau, including the

288   peripheral seas.

289

290   **RESULTS**

291   **Global patterns of gelatinous zooplankton biomass**

292   Our quantitative dataset (n = 91,765, 5° grid cells = 572) covers 33% of the total ocean area;

293   43% for the Northern Hemisphere and 23% for the Southern Hemisphere (Fig. 1, Table 2).

294   The global median, and geometric mean and geometric standard deviation of total GZ

295   biomass in the epipelagic ocean for the past 78 years were 0.81 mg C m^{-3}, and 0.53 ± 16.62

296   mg C m^{-3} (Table 1). Total GZ biomass varies >7 orders of magnitude across the ocean, with

297   minimum and maximum geometric means of 2 x10^{-4} and 2.3 x 10^3 mg C m^{-3} recorded within

298   the Indian South Subtropical Gyre and North Pacific Tropical Gyre provinces, respectively.

299   Within the major ocean basins, the geometric mean ranged from 0.01 in the South Indian

300   Ocean to 4.07 mg C m^{-3} in the North Pacific Ocean (Table 2). The highest standard deviation,

301   ±47.89, was recorded from the Arctic.

302

303   Our analysis shows that GZ are present across production gradients from eutrophic coastal

304   areas to oligotrophic oceanic subtropical gyres, and across temperature gradients from polar

305   to tropical regions. The top 10% of Longhurst provinces had geometric means of biomass >6

306   mg C m^{-3}: in the Alaska coastal downwelling (11.12 mg C m^{-3}), the north-western Atlantic

307   shelf (6.68 mg C m^{-3}) and the subarctic, tropical and subtropical North Pacific (6.14 – 14.21

308   mg C m^{-3}) (Appendix S6). Coastal and polar regions in the Northern Hemisphere generally

309　exhibited the highest average and maximum total GZ biomass values compared to those of

310　the open ocean and Southern Hemisphere (Fig. 1). Maximum total GZ biomass was recorded

311　along the east coast the USA (202,838 mg C m^{-3}), the central North Pacific (35,213 mg C m^{-}

312　^{3}), the Mediterranean (30,344 mg C m^{-3}), the boreal polar region (18,582 mg C m^{-3}) and the

313　shelf seas around the British Isles and Norway (14,262 mg C m^{-3}) (Fig. 1). While some of

314　these high biomass regions also exhibit high CV particularly around the coasts, indicating the

315　co-occurrence of high biomass and GZ blooms in space and time, on a global scale geometric

316　mean of biomass and CV were negatively correlated (r_s = -0.21, P < 0.05, n = 579)

317　suggesting that many low GZ biomass regions can also be highly influenced by occasional

318　blooms and sporadic patchiness. Lowest GZ biomass of <0.01 mg C m^{-3} was in oligotrophic

319　or iron-limited Southern Hemisphere regions, including Western Australia, Brazil, the

320　southern subtropical Indian Ocean and the sub-Antarctic.

321

322　When the three taxa are considered separately, the Thaliacea (n = 24,998) and Cnidaria (n =

323　57,663) are the most widely distributed (Fig. 2), and contributed the most to total GZ biomass

324　and abundance (Appendix S6). Ctenophores (n = 8,757) were sampled primarily from the

325　North Atlantic and to a lesser extent the tropical and subtropical North Pacific (Fig. 2). The

326　global geometric mean and geometric standard deviation of biomass for each phylum were

327　0.09 ± 20.53 mg C m^{-3} (calculated from 505 grid cells) for the Thaliacea, 4.43 ± 6.89 mg C

328　m^{-3} (511 grid cells) for the Cnidaria and 1.14 ± 24.55 mg C m^{-3} (227 grid cells) for the

329　Ctenophora.

330

331　All three taxa displayed similar latitudinal trends in the geometric mean of biomass (Fig. 3).

332　The minimum occurs around 20 - 30°S, then increases with latitude from the equatorial and

333　northern subtropical regions to a peak at around 50 - 60°N. Although data are sparse and

334   variable for the high latitudes, polar regions supported higher GZ biomass. Similarly, the low

335   number of observations for the Southern Hemisphere makes interpretation of biomass trends

336   south of 30 - 40° difficult to achieve with a high degree of confidence.

337

338   **Environmental drivers of Cnidaria, Ctenophora and Thaliacea biomass**

339   The combination of high spatial autocorrelation, low sample number for the Southern

340   Hemisphere and asymmetry in latitudinal trend between the north and south, may lead to

341   misrepresentation of global patterns. As a result, statistical analyses of environmental drivers

342   for biomass distributions were limited to the North Atlantic where more data are available.

343   Once spatial autocorrelation had been accounted for, significant relationships with Cnidaria,

344   Ctenophora and Thaliacea biomass only existed with DO and AOU. SST ($P < 0.05$) was a

345   significant explanatory variable for biomass of both Thaliacea and Cnidaria. PP ($P < 0.05$)

346   and distance from coast ($P < 0.05$) were specifically related to only Ctenophora and Cnidaria

347   biomass distribution respectively. Cnidarians, ctenophores and thaliaceans were found in a

348   broad range of DO concentrations from 2-8 ml O_2 L^{-1}, with significant linear trends for all

349   three taxa (Fig. 4 and 5). Significant relationships occurred between AOU and biomass for all

350   three GZ groups ($P < 0.05$) (Table 3). The partial residual plots showed that these

351   relationships, once the other environmental variables had been held constant, were positive

352   for all taxa (Fig. 5). All three GZ taxa were present across the full spectrum of sea surface

353   temperatures between 0 and 28°C. The linear trends between average biomass and SST were

354   positive for the Thaliacea ($P < 0.05$) and the Cnidaria ($P < 0.001$), but not significant for the

355   Ctenophora (Fig. 5, Table 3). There was a significant positive relationship between biomass

356   of the Ctenophora and PP ($P < 0.05$) (Fig. 5). Cnidaria biomass also increased with

357   decreasing distance from the coast. There were no significant relationships between biomass

358   and bathymetric depth, euphotic zone depth or chlorophyll *a*.

359

DISCUSSION

Gelatinous biomass in the global ocean

362   Global estimates of macrozooplankton, and in particular GZ biomass, are extremely rare and

363   are typically accompanied by a number of caveats, mainly relating to uneven spatial coverage

364   of available data across the globe, particularly in the Southern Hemisphere. Our biomass data

365   are significantly more variable than that found by Lynam *et al.* (2011) for the Irish Sea where

366   62 samples were required to reduce RSE to 5%. None of the 5° grid cells in this study had

367   observed data (not bootstrapped) with an RSE as low as 5%, even those with many thousands

368   of observations. This is most likely a result of the variation in sampling methodologies

369   (Appendix S3) and increased spatial extent of our data from a variety of ocean ecosystems.

370   Moriarty *et al.* (2012) reported a median biomass of 0.19 mg C m^{-3} for macrozooplankton >2

371   mm sampled from 0 - 350m depth, which is almost twice the depth range used in our analysis

372   (median 0.81 mg C m^{-3} in 0 - 200m depth) and therefore includes regions that sustain lower

373   GZ biomass. Direct comparisons with Lilley *et al.* (2011) are difficult, as their data are

374   expressed as g WW 100 m^{-3}, and more significantly, our spatial coverage is more widespread

375   and includes a high proportion of data from the open ocean including the Indian Ocean and

376   the mid-ocean regions of the North Atlantic and Pacific Oceans. Only 31% of the datasets in

377   Lilley *et al.* (2011) are oceanic and many of the other datasets are taken from estuaries, lakes

378   and enclosed seas of the Northern Hemisphere (e.g. Jellyfish Lake in Palau, Honjo Lake in

379   Japan) known to contain significant GZ blooms.

380

381   We calculate that cnidarians, ctenophores and thaliaceans contribute 92.0 %, 5.5% and 2.5%

382   to an estimated total global GZ biomass of 38.3 Tg C in the upper 200m of ocean (estimated

383   from our GZ geomean of 0.53 mg C m^{-3} and assuming global ocean area = 361,900,000 km^{2}).

16

384   Estimates of global-averaged phytoplankton and zooplankton median biomass are 56 mg C

385   m^{-3} (Boyce *et al.*, 2010, where mg Chl *a* is converted to C using median Chl:C of 0.01

386   according to Behrenfeld *et al.*, 2005) and 4.18 mg C m^{-3} (Strömberg *et al.*, 2009: Table A1,

387   where biomass is modelled from primary production and transfer efficiencies), respectively.

388   These order of magnitude differences between successive trophic levels (phytoplankton to

389   zooplankton to GZ) are expected assuming classic food web structure and transfer

390   efficiencies (Strömberg *et al.*, 2009). Based on two (thaliaceans) or three (cnidarians,

391   ctenophores) trophic levels, 10% trophic transfer efficiency and 30 - 60 Pg C of primary

392   production available (Watson *et al.*, 2013), we estimate that < 0.01 - 12 % of the mean annual

393   global primary production is required to support the estimated global GZ biomass reported in

394   our study.

395

396   Our global maps and analyses highlight the truly global distribution of GZ in the world's

397   oceans, from the productive coastal regions where biomass is greatest, to the open ocean and

398   oligotrophic regions. Nevertheless, clear spatial patterns in biomass are evident. While the

399   observed latitudinal trends in Cnidaria, Ctenophora and Thaliacea biomass are in broad

400   agreement with that reported for other macrozooplankton (Moriarty *et al.*, 2012) and

401   crustacean mesozooplankton (see Hernández-León & Ikeda, 2005: Fig. 1; Strömberg *et al.*,

402   2009: Fig. 2), the differential between the GZ biomass in the Southern and Northern

403   Hemispheres is unclear. It may result from low spatial coverage of quantitative samples,

404   particularly in the Southern Ocean where GZ are known to be abundant, but were unavailable

405   to JEDI. It may reflect zooplankton food availability for GZ predators; Hernández-León &

406   Ikeda (2005) suggested that higher zooplankton biomass at 10 - 20°N compared with the

407   minimal biomass at equivalent latitudes south of the equator was attributed to the productive

408   north-equatorial waters of the Atlantic Ocean. The reduced coastline in the Southern

409   Hemisphere may be significant for scyphozoan and some hydrozoan jellyfish that require

410   shallow-water hard surfaces for their benthic polyps to inhabit as part of the cnidarian life

411   cycle. Finally, lower human impact (e.g. eutrophication, fishing pressure, contaminant loads)

412   on marine ecosystems in the Southern Hemisphere relative to the Northern Hemisphere

413   (Halpern *et al*., 2008) may also influence GZ biomass, as suggested by Purcell *et al*. (2007).

414

Environmental drivers of gelatinous biomass

416   Our analyses suggest that the large-scale spatial trends in the baseline distribution of GZ

417   biomass in the Atlantic are significantly related to several environmental variables,

418   particularly SST, DO and primary production. Although data are currently limited, these

419   trends may apply more generally on global scales but interact synergistically with additional

420   environmental variables (e.g. riverine nutrient inputs) on local and regional scales (Condon *et*

421   *al*., 2013).

422

423   In agreement with Lilley *et al*. (2011), we found no significant correlation with chlorophyll *a*,

424   although there was a significant relationship between Ctenophora biomass and primary

425   production. The role of primary production in shaping faunal biomass is a common theme

426   across several taxa and terrestrial and marine ecosystems (Hernández-Leon & Ikeda, 2005:

427   Jennings *et al*., 2008; Fierer *et al*., 2009), and while correlations with PP might be expected

428   as it reflects rates of carbon fixation by the entire autotrophic community that ultimately

429   sustains GZ biomass, it was not a particularly important driver of GZ biomass. The result for

430   chlorophyll *a* is as expected as chlorophyll *a* indicates the net difference between growth and

431   removal processes such as viral lysis and grazing.

432

433   There was a broad trend of increasing biomass with increasing DO for all GZ taxa, at the

434   lower end of this scale relatively high GZ biomass was still distributed in regions of

435   persistent low DO and hypoxia. Furthermore, high ctenophore biomass was associated with

436   regions of increased AOU, indicating a connection between GZ biomass and increased

437   community respiration (del Giorgio & Duarte, 2002). These results further indicate that GZ

438   may be able to persist in regions unavailable to other pelagic organisms, such as fish, which

439   are intolerant of low DO conditions (<4 mg O_2 L^{-1}). They are also consistent with previous

440   studies that suggest several coastal bloom-forming and oceanic GZ species, including *Aurelia*

441   spp., *Chrysaora quinquecirrha*, *Cyanea capillata*, *Mnemiopsis leidyi* and *Pleurobrachia*

442   *bachei*, tolerate hypoxic (30% air saturation, <2 mg O_2 L^{-1}) and even severely hypoxic (<0.5

443   mg O_2 L^{-1}) conditions (Thuesen *et al*., 2005). Furthermore, extreme abundances of the

444   scyphozoan *Crambionella orsini* have been observed within the Oxygen Minimum Zone

445   (<0.5 mg O_2 L^{-1}) on the upper slopes off the coast of Oman (Billett *et al.*, 2006). Thus, our

446   findings show a general trend of increasing GZ biomass with increasing DO levels but

447   evidence that high GZ biomass can occur in areas of very low DO. The mechanisms by

448   which GZ can persist under these conditions are not clear and warrant further investigation,

449   but could be related to the unique allometric (e.g. relatively low carbon demand relative to

450   individual size) and intracellular physiological characteristics (e.g. anaerobic pathways)

451   associated with adopting a gelatinous body plan (Pitt *et al*., 2013). GZ have been shown

452   experimentally to exhibit comparatively low oxygen thresholds for hypoxia-driven mortality

453   (Vaquer-Sunyer & Duarte, 2008).

454

455   Our analysis for the North Atlantic revealed a significant positive linear relationship between

456   Cnidaria and Thaliacea biomass and SST. This agrees with several other studies that suggest

457   increased cnidarian and thaliacean biomass is associated with warmer SST (e.g. the

458   Mediterranean, Kogovšek *et al.*, 2010; the North Atlantic, Gibbons & Richardson, 2009),

459   although trends are not universal and species- and geographical-range specific differences in

460   temperature tolerance will drive differences on local and regional scales (see Zhang *et al.*,

461   2012). In cnidarians, warmer temperatures generally increase rates of asexual reproduction of

462   the benthic polyp phase of the life cycle (Lucas *et al.*, 2012), which could increase production

463   of medusae. For thaliaceans, the mechanisms might also be indirectly driven by SST as

464   generation times and reproductive output are affected by temperature and food availability

465   (Lucas & Dawson, 2014). In Antarctica higher salp abundances are observed during warmer

466   years with low sea ice owing to the higher proliferation of small phytoplankton cells versus

467   diatoms relative to colder years, which likely reflects their ability to efficiently utilise very

468   small cells <2 µm at high filtration rates (Sutherland *et al.*, 2010). Thaliaceans are also

469   prevalent in oligotrophic subtropical gyres where small cells contribute greatly to primary

470   production or have increased in biomass.

471

472   The negative relationship of Cnidarian biomass with distance from coast likely reflects their

473   life history. Members of the Class Scyphozoa (e.g. *Aurelia* spp., *Cyanea* spp., *Chrysaora*

474   spp.) dominate cnidarian biomass, the majority of which have a metagenic life cycle that

475   includes a perennial polyp found attached to natural and artificial substrata in shallow coastal

476   habitats. Owing to the short lifespan of most cnidarian medusae, the abundance of the adult

477   population depends on the local polyp populations (Lucas *et al.*, 2012).

478

479   **Concluding remarks and future consequences of GZ biomass**

480   The main drivers of ocean-scale spatial distribution of GZ biomass are SST, DO and AOU;

481   distance from coast and PP are significant drivers only for the Cnidaria and Ctenophora,

482   respectively. Nonetheless, the presence of gelatinous taxa across the complete spectra of

483   oxygen, temperature and productivity values suggest that the independent evolution of the

484   gelatinous body plan has delivered a range of phyla that are able to adapt to a wide range of

485   ecological niches, demonstrated by the truly global presence of gelatinous zooplankton.

486   Many of the locations that sustain high GZ biomass have experienced increases in SST and

487   reduced DO over the last three decades at rates greater than the global average, which,

488   together with other climate- and anthropogenic-driven impacts (Halpern *et al.*, 2008), is

489   expected to continue. Marked shifts in autotrophic assemblages and primary production are

490   also predicted to change with large-scale global processes (Blanchard *et al.*, 2012). While the

491   mechanisms are untested, it has been hypothesized that changes in these physical and

492   chemical factors will affect the ecology and global distribution of GZ favouring their future

493   proliferation (Purcell *et al.*, 2007).

494

495   Our spatial analysis is an essential first step in the establishment of a truly appropriate and

496   uniformly consistent parameterisation of gelatinous presence from which future trends can be

497   assessed and hypotheses tested, particularly those relating multiple regional and global

498   drivers on GZ biomass. It complements the recent temporal meta-analysis of Condon *et al.*

499   (2013) in which global GZ populations (particularly cnidarian medusae) were shown to

500   exhibit oscillations over multi-decadal timescales centred round a baseline. If GZ biomass

501   does increase in the future, particularly in the Northern Hemisphere, this may influence

502   zooplankton and phytoplankton abundance and biodiversity, having a knock-on effect on

503   ecosystem functioning, biogeochemical cycling (Condon *et al.*, 2011; Lebrato *et al.*, 2012)

504   and fish biomass (Pauly *et al.*, 2009). The continued development of JeDI and a re-analysis

505   several decades from now will enable science to determine whether GZ biomass and

506   distribution alters as a result of anthropogenic climate change.

507

519

520
521 **REFERENCES**

522 1. Beaugrand, G., Edwards, M. & Legendre, L. (2010) Marine biodiversity, ecosystem

523 functioning, and carbon cycles. *Proceedings of the National Academy of Sciences USA*,

524 **107**, 10120-10124.

525 2. Behrenfeld, M.J., Falkowski, P.G. (1997) Photosynthetic rates derived from satellite-

526 based chlorophyll concentration. *Limnology and Oceanography,* **42**, 1-20.

527 3. Behrenfeld, M.J., Boss, E., Siegel, D.A & Shea, D.M. (2005) Carbon-based ocean

528 productivity and phytoplankton physiology from space. *Global Biogeochemical Cycles*,

529 **19**, GB1006, doi:10.1029/2004GB002299.

530 4. Billett, D.S.M., Bett, B.J., Jacobs, C.L., Rouse, I.P. & Wigham, B.D. (2006) Mass

531 deposition of jellyfish in the deep Arabian Sea. *Limnology and Oceanography*, **51**, 2077-

532 2083.

533 5. Bivand, R.S., Pebesma, E.J, Gomez-Rubio, V. (2008) Applied spatial data analysis with

534   R. Springer, New York. 374 pp.

535 6. Blanchard, J.L., Jennings, S., Holmes, R., Harle, J., Merino, G., Icarus Allen, J., Holt, J.,

536   Dulvy, N.K. & Barange, M. (2012) Potential consequences of climate change on primary

537   production and fish production in large marine ecosystems. *Philosophical Transactions of*

538   *the Royal Society, Series B*, **367**, 2979-2989.

539 7. Brotz, L., Cheung, W.W.L., Kleisner, K., Pakhomov, E. & Pauly, D. (2012) Increasing

540   jellyfish populations: trends in Large Marine Ecosystems. *Hydrobiologia*, **690**, 3-20.

541 8. Cheung, W.W.L., Close, C., Lam, V., Watson, R. & Pauly, D. (2008) Application of

542   macroecological theory to predict effects of climate change on global fisheries potential.

543   *Marine Ecology Progress Series*, **365**, 187-197.

544 9. Cheung, W.W.L., Lam, V.W.Y., Sarmiento, J.L., Kearney, K., Watson, R., Zeller, D. &

545   Pauly, D. (2010) Large-scale redistribution of maximum fisheries catch potential in the

546   global ocean under climate change. *Global Change Biology*, **16**, 24-35.

547 10. Condon, R.H., Steinberg, D.K., del Giorgio, P.A., Bouvier, T.C., Bronk, D.A., Graham,

548   W.M. & Ducklow, H.W. (2011) Jellyfish blooms result in a major microbial respiratory

549   sink of carbon in marine systems. *Proceedings of the National Academy of Sciences of the*

550   *United States of America*, **108**, 10225-10230.

551 11. Condon, R.H., Graham, W.M., Duarte, C.M., Pitt, K.A., Lucas, C.H., Haddock, S.H.D.,

552   Sutherland, K.R., Robinson, K.L., Dawson, M.N., Decker, M.B., Mills, C.E., Purcell,

553   J.E., Malej, A., Mianzan, H., Uye, S.-I., Gelcich, S. & Madin, L.P. (2012) Questioning

554   the rise of gelatinous zooplankton in the World's oceans. *Bioscience*, **62**, 160-169.

555 12. Condon, R.H., Duarte, C.M., Pitt, K.A., Robinson, K.L., Lucas, C.H., Sutherland, K.R.,

556   Mianzan, H.W., Bogeberg, M., Purcell, J.E., Decker, M.B., Uye, S-I., Madin, L.P.,

557   Brodeur, R.D., Haddock, S.H.D., Malej, A., Parry, G.D., Erikson, E., Quinoñes, J., Acha,

558   M., Harvey, M., Arthur, J.M. & Graham, W.M. (2103) Recurrent jellyfish blooms are a

559   consequence of global oscillations. *Proceedings of the National Academy of Science of*

560   *the United States of America*, **110**, 1000-1005.

561   13. Currie, D.J. & Fritz, J.T. (1993) Global patterns of animal abundance and species energy

562   use. *Oikos*, **67**, 56-68.

563   14. del Giorgio, P.A. & Duarte, C.M. (2002) Respiration in the open ocean. *Nature*, **420**, 379-

564   384.

565   15. Dormann, C.F., McPherson, J.M., Araujo, M.B., Bivand, R., Bolliger, J., Carl, G., Davies,

566   R.G., Hirzel, A., Jetz, W., Kissling, W.D., Kuhn, I., Ohlemuller, R., Peres-Neto, P.R.,

567   Reineking, B., Schroder, B., Schurr, F.M. & Wilson, R. (2007) Methods to account for

568   spatial autocorrelation in the analysis of species distributional data: a review. *Ecography,*

569   **30**, 609-628.

570   16. Field, C.B., Behrenfeld, M.J., Randerson, J.T. & Falkowski, P. (1998) Primary production

571   of the biosphere: integrating terrestrial and oceanic components. *Science*, **281**, 237-240.

572   17. Fierer, N., Strickland, M.S., Liptzin, D., Bradford, M.A. & Cleveland, C. (2009) Global

573   patterns in belowground communities. *Ecology Letters*, **12**, 1238-1249.

574   18. Gibbons, M.J. & Richardson, A.J. (2009) Patterns of jellyfish abundance in the North

575   Atlantic. *Hydrobiologia*, **616**, 51-65.

576   19. Halpern, B.S., Walbridge, S., Selkoe, K.A., Kappel, C.V., Micheli, F., Agrosa, C.D.,

577   Bruno, J.F., Casey, K.S., Ebert, C., Fox, H.E., Fujita, R., Heinemann, D., Lenihan, H.S.,

578   Madin, E.M.P, Perry, M.T., Selig, E.R., Spalding, M., Steneck, R. & Watson, R. (2008) A

579   global map of human impact on marine ecosystems. *Science*, **319**, 948-952.

580   20. Hendriks, I.E., Duarte, C.M. & Heip, C.H.R. (2006) Biodiversity research still grounded.

581   *Science*, **312**, 1715.

24

582   21. Hernández-León, S. & Ikeda, T. (2005) A global assessment of mesozooplankton
583   respiration in the ocean. *Journal of Plankton Research*, **27**, 153-158.

584   22. Hese, S., Lucht, W., Schmullius, C., Barnsley, M., Dubayah, R., Knorr, D., Neumann, K.,
585   Riedel, T. & Schröter, K. (2005) Global biomass mapping for an improved understanding
586   of the CO_2 balance – the Earth observation mission Carbon-3D. *Remote Sensing of*
587   *Environment*, **94**, 94-104.

588   23. Houghton, J.D.R., Doyle, T.K., Wilson, M.W., Davenport, J. & Hays, G.C. (2006)
589   Jellyfish aggregations and leatherback turtle foraging patterns in a temperate coastal
590   environment. *Ecology*, **87**, 1967-1972.

591   24. Huston, M.A. & Wolverton, S. (2009) The global distribution of net primary production:
592   resolving the paradox. *Ecological Monographs*, **79**, 343-377.

593   25. IPCC (Intergovernmental Panel on Climate Change) (2007) Summary for policymakers.
594   In: Solomon, S., Qin, D., Manning, M., Chen, Z. *et al.* (eds) Climate change 2007: the
595   physical science basis. Contribution of Working Group I to the Fourth Assessment Report
596   of the Intergovernmental Panel on Climate Change. Cambridge University Press, New
597   York, p 1–18.

598   26. Jennings, S., Mélin, F., Blanchard, J.L., Forster, R.M., Dulvy, N.K. & Wilson, R.W.
599   (2008) Global-scale predictions of community and ecosystem properties from simple
600   ecological theory. *Proceedings of the Royal Society B*, **275**, 1375-1383.

601   27. Jones, D.O.B., Yool, A., Wei, C-L., Henson, S.A., Ruhl, H.A., Watson, R.A. & Gehlen,
602   M. (in press) Global reductions in seafloor biomass in response to climate change. *Global*
603   *Change Biology*

604   28. Kogovšek, T., Bogunović, B. & Malej, A. (2010) Recurrence of bloom-forming
605   scyphomedusae: wavelet analysis of a 200-year time series. *Hydrobiologia*, **645**, 81-96.

606   29. Lebrato, M., Pitt, K.A., Sweetman, A.K., Jones, D.O.B., Cartes, J.E., Oschlies, A.,

607   Condon, R.H., Molinero, J.C., Adler, L., Gaillard, C., Lloris, D. & Billett, D.S.M. (2012)

608   Jelly-falls historic and recent observations: a review to drive future research directions.

609   *Hydrobiologia*, **690**, 227-245.

610   30. Lilley, M.K.S., Beggs, S.E., Doyle, T.K., Hobson, V.J., Stromberg, K.H.P. & Hays, G.C.

611   (2011) Global patterns of epipelagic gelatinous zooplankton biomass. *Marine Biology*,

612   **158**, 2429-2436.

613   31. Lucas, C.H. & Dawson, M.N. (2014) What are jellyfishes and thaliaceans and why do

614   they bloom? In: Pitt, K.A. & Lucas, C.H. (eds) *Jellyfish Blooms*, Springer. pp 9 - 44. doi:

615   10.1007/978-94-007-7015-7

616   32. Lucas, C.H., Pitt, K.A., Purcell, J.E., Lebrato, M. & Condon, R.H. (2011) What's in a

617   jellyfish? Proximate and elemental composition and biometric relationships for use in

618   biogeochemical studies. *Ecology*, **92**, 1704.

619   33. Lucas, C.H., Graham, W.M. & Widmer, C. (2012) Jellyfish life histories: the role of

620   polyps in forming and maintaining scyphomedusa populations. *Advances in Marine*

621   *Biology*, **63**, 33-196.

622   34. Lynam, C.P, Lilley, M.K.S., Bastian, T., Doyle, T.K., Beggs, C.E. & Hays, G.C. (2011)

623   Have jellyfish in the Irish Sea benefited from climate change and overfishing? *Global*

624   *Change Biology*, **17**, 767-782.

625   35. Moriarty, R., Buitenhuis, E.T., Le Quéré, C. & Gosselin, M.-P. (2012) Distribution of

626   known macrozooplankton abundance and biomass in the global ocean. *Earth System*

627   *Science Data Discussions*, **5**, 187-220.

628   36. Moritz, C. & Agudo, R. (2013) The future of species under climate change. Resilience or

629   decline? *Science*, **341**, 504-508.

630   37. Pauly, D., Graham, W., Libralato, S., Morissette, L. & Palomares, M.L.D. (2009)

631   Jellyfish in ecosystems, online databases, and ecosystem models. *Hydrobiologia*, **616**, 67-

632   85.

633   38. Pitt, K.A., Duarte, C.M., Lucas, C.H., Sutherland, K.R., Condon, R.H., Mianzan, H.,

634   Purcell, J.E., Robinson, K.R., Uye, S.-I. (2013) Jellyfish body plans provide allometric

635   advantages beyond low carbon content. *PLoS ONE,* **8(8)**, e72683.

636   39. Purcell, J.E., Uye, S.-I. & Lo, W.-T. (2007) Anthropogenic causes of jellyfish blooms and

637   their direct consequences for humans: a review. *Marine Ecology Progress Series*, **350**,

638   153-174.

639   40. Rex, M.A., Etter, R.J., Morris, J.M., Crouse, J., McClain, C.R., Johnson, N.A., Stuart,

640   C.T., Deming, J.W., Thies, R. & Avery, R. (2008) Global bathymetric patterns of

641   standing stock and body size in the deep-sea benthos. *Marine Ecology Progress Series*,

642   **317**, 1-8.

643   41. Richardson, A.J. (2008) In hot water: zooplankton and climate change. *ICES Journal of*

644   *Marine Science*, **65**, 279-295.

645   42. Robinson, L.M., Elith, J., Hobday, A.J., Pearson, R.G., Kendall, B.E., Possingham, H.P.

646   & Richardson, A.J. (2011) Pushing the limits in marine species distribution modelling:

647   lessons from the land present challenges and opportunities. *Global Ecology and*

648   *Biogeography*, **20**, 789-802.

649   43. Ricciardi, A. & Bourget, E. (1999) Global patterns of macroinvertebrate biomass in

650   marine intertidal communities. *Marine Ecology Progress Series*, **185**, 21-35.

651   44. Strömberg, K.H.P., Smyth, T.J., Allen, J.I., Pitois, S. & O'Brien, T.D. (2009) Estimation

652   of global zooplankton biomass from satellite ocean colour. *Journal of Marine Systems*,

653   **78**, 18-27.

654   45. Sutherland, K.R., Madin, L.P. & Stocker, R. (2010) Filtration of submicrometer particles

655   by pelagic tunicates. *Proceedings of the National Academy of Science of the United States*

656   *of America*, **107**, 15129-15134.

657   46. Thuesen, E.V., Rutherford, L.D., Brommer, P.L., Garrison, K., Gutowska, M.A. &

658   Towanda, T. (2005) Intragel oxygen promotes hypoxia tolerance of scyphomedusae.

659   *Journal of Experimental Biology*, **208**, 2475-2482.

660   47. Tittensor, D.T., Mora, C., Jetz, W., Lotze, H.K., Ricard, D., Berghe, E.V. & Worm, B.

661   (2010) Global patterns and predictors of marine biodiversity across taxa. *Nature*, **466**,

662   1098-1101.

663   48. Vaquer-Sunyer, R. & Duarte, C.M. (2008) Thresholds of hypoxia for marine biodiversity.

664   *Proceedings of the National Academy of Sciences of the United States of America,* **105**,

665   15452–15457.

666   49. Watson, R., Zeller, D. & Pauly, D. (2013) Primary production demands of global

667   fisheries. *Fish and Fisheries*, doi: 10.1111/faf.12013.

668   50. Wei, C-L., Rowe, G.T., Escobar-Briones, E., Boetius, A., Soltwedel, T., Caley, M.J.,

669   Soliman, Y., Huettmann, F., Qu, F., Yu, Z., Pitcher, C.R., Haedrich, R.L., Wicksten,

670   M.K., Rex, M.A., Baguley, J.G., Sharma, J., Danovaro, R., MacDonald, I.R., Nunnally,

671   C.C., Deming, J.W., Montagna, P., Lévesque, M., Weslawski, J.M., Wlodarska-

672   Kowalczuk, M., Ingole, B.S., Bett, B.J., Billett, D.S.M., Yool, A., Bluhm, B.A., Iken, K.

673   & Narayanaswamy, B.E. (2010) Global patterns and predictions of seafloor biomass

674   using random forests. *PLoS ONE*, **5(12)**, e15323.

675   51. Zhang, F., Sun, S., Jin, X.S. & Li, C.L. (2012) Associations of large jellyfish distributions

676   with temperature and salinity in the Yellow Sea and East China Sea. *Hydrobiologia*, **690**,

677   81-96.

678

679 **BIOSKETCH**

Catherine Hollyhead is currently studying for an EngD at the University of Southampton.

Cathy Lucas, Rob Condon, Carlos Duarte, Monty Graham, Kelly Robinson and Kylie Pitt are

all members of an NCEAS working group titled "Global expansion of jellyfish blooms:

Magnitude, causes and consequences" http://www.nceas.ucsb.edu/projects/12479. Mark

Schildauer and Jim Regertz are or were based at NCEAS. Daniel Jones is a researcher in

deep-sea biology, with a particular interest in the reservoirs and fate of global gelatinous

zooplankton biomass. Author contributions: CHL, CJH, RHC and DOBJ wrote the article;

CJH, CHL, RHC & CMD designed the study; DOBJ & CJH analysed the data and prepared

the figures; WMG, KLR, KAP, CHL & RHC compiled and assembled the datasets in JeDI,

MS & JR provided database technical support at NCEAS. All authors commented on drafts

of the manuscript and contributed substantially to revisions.

680

SUPPORTING INFORMATION

Appendix S1. Maps of the Jellyfish Database Initiative (JeDI) database.

Appendix S2. Template used to gather data for entry into the Jellyfish Database Initiative

(JeDI) database.

Appendix S3. Relative contribution of different sampling methods used to collect

quantitative gelatinous zooplankton data.

Appendix S4. Published biometric equations and body composition ratios used to convert

gelatinous zooplankton species abundance into carbon biomass.

Appendix S5. Relative standard errors (RSE) in the mean as a function of the number of

observations within a 5° grid cell.

Appendix S6. Summary of environmental and gelatinous zooplankton data for each

Longhurst province.

TABLES

Table 1. Summary of descriptive statistics of global biomass (mg C m^{-3}) of medusae (phylum Cnidaria), ctenophores (phylum Ctenophora) and pelagic tunicates (phylum Chordata), based upon 5° gridded data comprising 91,765 samples taken from the Jellyfish Database Initiative (JeDI). GZ = gelatinous zooplankton; n = number of observations; Mean = geometric mean for biomass and arithmetic mean for all other variables; SD = standard deviation; P(SWilk) = probability of a normal distribution based on a Kolmogorov-Smirnov test; SST = sea surface temperature; DO = dissolved oxygen; AOU = apparent oxygen utilisation.

Variable	n	Mean ± SD	Maximum	Median	Skewness	P(SWilk)
Total GZ biomass (mg C m^{-3})	572	0.53 ±16.62	2292.06	0.81	17.61	<0.001
Bathymetric depth (m)	579	3,121 ±1,921	6,040	3,778	0.49	<0.001
Chlorophyll *a* (mg m^{-3})	492	0.57 ±1.17	8.50	0.19	4.05	<0.001
SST (^{o}C)	492	20.02 ±9.54	32.08	24.07	-0.98	<0.001
DO (ml L^{-1})	500	4.69 ±1.30	7.90	4.65	0.29	<0.001
AOU (ml L^{-1})	495	1.32 ±0.78	4.17	1.06	1.16	<0.001
Euphotic zone depth (m)	575	74.9 ±28.3	142.4	77.7	-0.03	<0.001
Primary production (g C m^{-2} yr^{-1})	575	229.2 ±235.5	1593.6	154.0	2.80	<0.001
Distance from coast (km)	579	623 ± 621	5,878	465	1.80	<0.001

681

Table 2. The geometric mean and geometric standard deviation (SD) of total GZ biomass

(mg C m^{-3}) for each ocean basin and the Mediterranean Sea (Med). The calculations were

performed upon the allocated 5° grid cells from the associated Longhurst province with the

equator as the north-south divide. For each ocean basin and sea, the number of 5° grid cells

and the percentage cover this represents, for which quantitative data were available and from

which the calculations were made is also shown.

	Arctic	North Atlantic	South Atlantic	Med	North Pacific	South Pacific	North Indian	South Indian	Southern
Percentage cover	16%	80%	34%	59%	39%	14%	82%	39%	2%
Number of grid cells	46	140	57	10	129	51	49	94	3
Mean (mg C m^{-3})	1.38	1.61	0.17	0.22	4.07	0.37	0.13	0.01	3.63
SD (mg C m^{-3})	47.98	7.53	6.60	5.48	7.00	8.58	3.11	6.72	1.76

Table 3. Generalized-linear model (GLM) and spatial linear model (SLM) results for minimal adequate models using North Atlantic data. Numbers indicate t-values (GLM) or z-values (SLM), asterisks indicate significance of individual predictors: * $p < 0.05$; ** $p < 0.01$; *** $p < 0.001$ and ns is not significant. Coefficients are presented in parentheses. AIC = Akaike information criterion, SST = sea surface temperature, DO = dissolved oxygen, AOU = apparent oxygen utilisation. Moran's I is calculated on the model residuals.

	Ctenophores		Thaliaceans		Cnidarians	
	GLM	SLM	GLM	SLM	GLM	SLM
Bathymetric depth						
Chlorophyll *a*						
SST			(0.17) 5.36***	(0.13) 3.76***	(0.06) 2.22*	(0.05) 2.43*
DO	(0.29) 3.60***	(0.24) 2.28*	(1.68) 5.64***	(1.28) 3.98***	(0.55) 2.71**	(0.58) 2.82**
AOU	(0.46) 4.27***	(0.34) 2.70**	(1.63) 5.29***	(1.24) 4.05***	(0.46) 2.09*	(0.49) 2.20*
Euphotic zone depth						
Primary production	(0.001) 2.69**	(0.001) 2.71**				
Distance from coast					(-0.001) -2.24*	(-0.001) -2.30*
R^2 (GLM) / Pseudo R^2 (SLM)	0.27	0.26	0.29	0.19	0.09	0.35
AIC	144.69	143.18	179.94	176.64	103.74	104.86
Moran's I	0.139*	0.016 ns	0.193**	0.022 ns	0.087 ns	0.007 ns

FIGURE LEGENDS

Figure 1. Maps of 5° grid cells data of sampled total gelatinous zooplankton plotted over Longhurst provinces of (a) number of sample observations; (b) maximum biomass (mg C m^{-3}); (c) geometric mean of biomass (mg C m^{-3}); and (d) coefficient of variation using the arithmetic mean of biomass. Areas where there are no observations are indicated by light blue (sea).

Figure 2. Maps of 5° grid cells data of geometric mean biomass (mg C m^{-3}) plotted over Longhurst Provinces of (a) Cnidaria; (b) Ctenophora; and (c) Thaliacea. Areas where there are no observations are indicated by light blue (sea).

Figure 3. Latitudinal trends of global biomass of (a) Cnidaria; (b) Ctenophora; and (c) Thaliacea. Trends indicated by fit from single-variable linear models (lines with grey area indicating 95% confidence limits). Note log (base 10) scale on y axis.

Figure 4. Scatterplots showing significant relationships between biomass of Ctenophora (a-c), Thaliacea (d-f) and Cnidaria (g-j) and environmental variables in the North Atlantic. DO = dissolved oxygen, AOU = apparent oxygen utilisation, SST = sea surface temperature, PP = primary production. Note log (base 10) scale on y axis.

Figure 5. Partial residual plots for the predictors of the minimum adequate SLM biomass of Ctenophora (a-c), Thaliacea (d-f) and Cnidaria (g-j) and environmental variables in the North Atlantic. Plots show the individual effects of: DO = dissolved oxygen, AOU = apparent oxygen utilisation, SST = sea surface temperature, PP = primary production, Euphotic depth = euphotic zone depth. A partial residual plot is a plot of $r_i + b_k*i_k$ vs. x_{ik}, where r_i is the
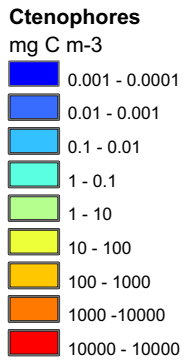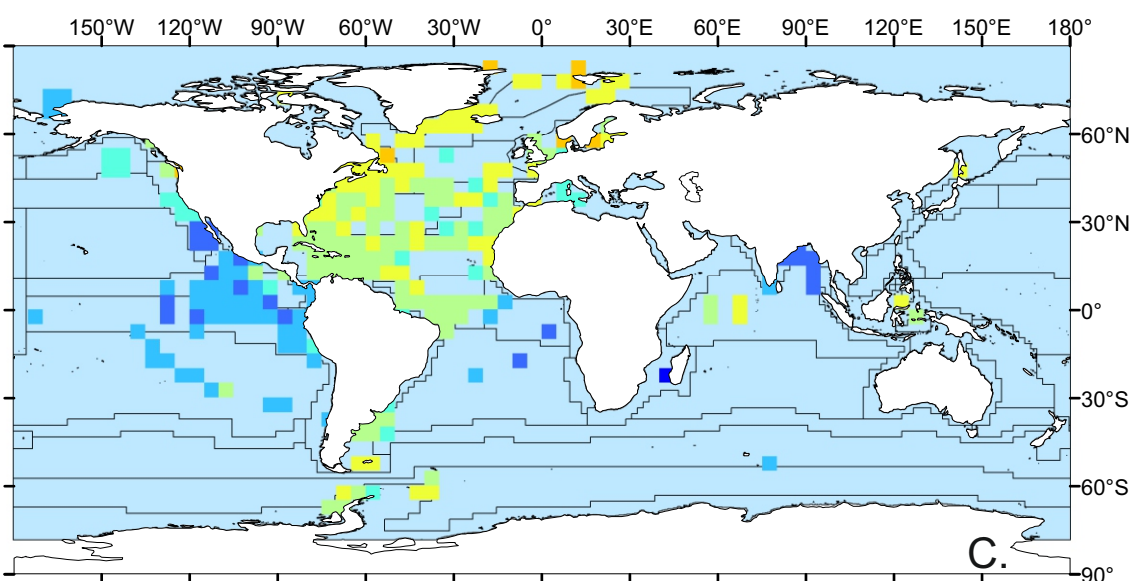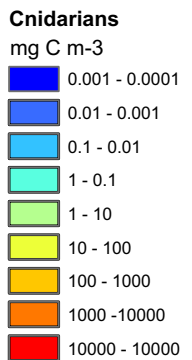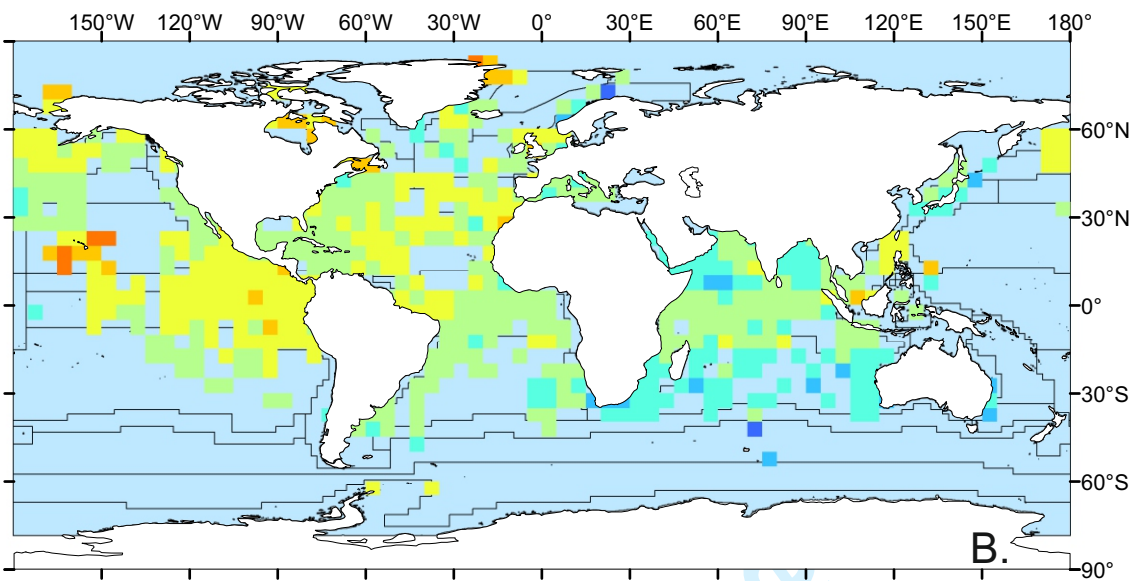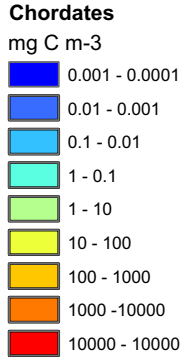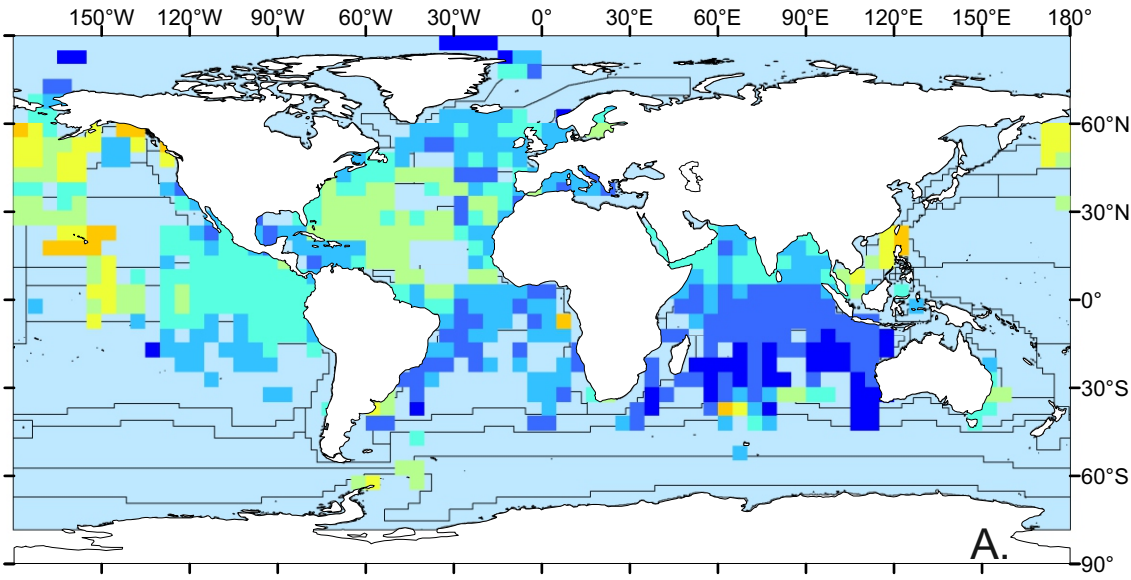
33

ordinary residual for the i-th observation, x_{ik} is the i-th observation of the k-th predictor and b_k

is the regression coefficient estimate for the k-th predictor. Regression lines indicate partial

fits.

A.

No. observations
- 0
- 1 - 10
- 10 - 50
- 50 - 100
- 100 - 250
- 250 - 1,000
- 1,000 - 2,500
- 2,500 - 5,000
- 5,000 - 10,000

B.

Max. Biomass
mg C m-3
- 0.001 - 0.0001
- 0.01 - 0.001
- 0.1 - 0.01
- 1 - 0.1
- 1 - 10
- 10 - 100
- 100 - 1000
- 1000 -10000
- 10000 - 10000

C.

Mean Biomass
mg C m-3
- 0.001 - 0.0001
- 0.01 - 0.001
- 0.1 - 0.01
- 1 - 0.1
- 1 - 10
- 10 - 100
- 100 - 1000
- 1000 -10000
- 10000 - 10000

D.

Coeff. Variation
- 0.3 - 1
- 1 - 1.5
- 1.5 - 2
- 2 - 5
- 5 - 10
- 10 - 25
- 25 - 50
- 50 - 100
- >100

A. Cnidaria

Biomass, g

Latitude, °

B. Ctenophora

Biomass, g

Latitude, °

C. Thaliacea

Biomass, g

Latitude, °

A. Ctenophora
B. Ctenophora
C. Ctenophora
D. Thaliacea
E. Thaliacea
F. Thaliacea
G. Cnidaria
H. Cnidaria
I. Cnidaria
J. Cnidaria